

On Verdigris, Part II: Synthesis of the 2-1-5 Phase, $\text{Cu}_3(\text{CH}_3\text{COO})_4(\text{OH})_2 \cdot 5\text{H}_2\text{O}$, by long-term crystallisation from aqueous solution at room temperature

- Supporting Information -

Sebastian Bette,^{a,*} Reinhard K. Kremer,^a Gerhard Eggert,^b and Robert E. Dinnebier^a

^aMax Planck Institute for Solid State Research, Heisenbergstr. 1, 70569 Stuttgart, Germany

^bState Academy of Art and Design, Am Weißenhof 1, 70191 Stuttgart

Additional Tables and Figures

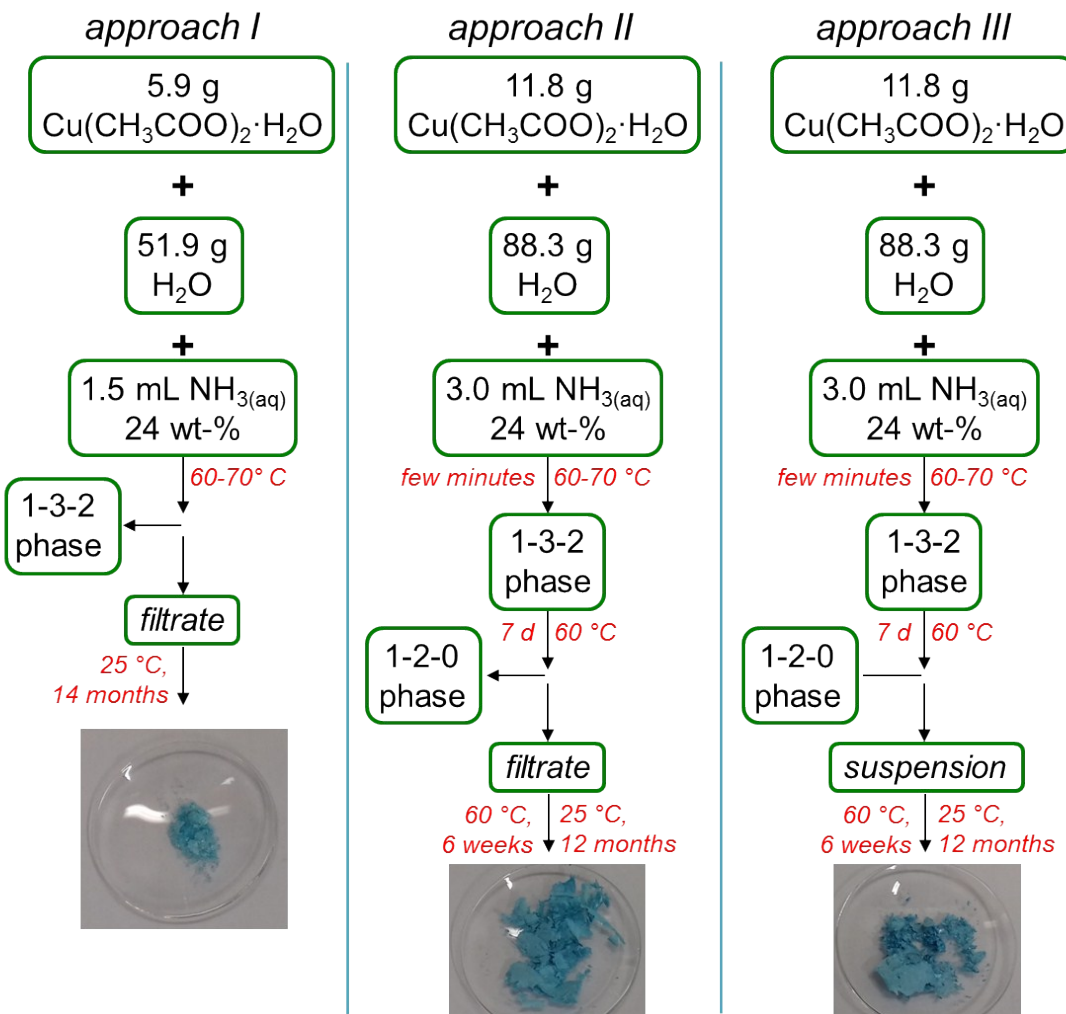


Figure S 1. Reaction scheme of the long-term synthesis approaches for new verdigris phases including photographs of the solid products.

Table S 1. Crystallographic and Rietveld Refinement data of the 2-1-5 phase ($\text{Cu}_3(\text{CH}_3\text{COO})_4(\text{OH})_2 \cdot 5\text{H}_2\text{O}$) at ambient conditions.

compound name	2-1-5 phase
molecular formula	$2\text{Cu}(\text{CH}_3\text{COO})_2 \cdot 1\text{Cu}(\text{OH})_2 \cdot 5\text{H}_2\text{O}$
sum formula	$\text{C}_8\text{H}_{24}\text{Cu}_3\text{O}_{15}$
molecular weight (g/mol)	550.895
space group	$P2_1/c$ (14)
Z	4
a /Å	12.4835(2)
b /Å	14.4246(2)
c /Å	10.7333(1)
α /°	90
β /°	102.871(1)
γ /°	90
V /Å ³	1884.18(5)
ρ_{calc} / g · cm ⁻³	1.94
Wavelength / Å	1.5406
R-p /% *	1.42
R-wp /% *	1.62
R- F^2 /% *	0.67
starting angle (° 2θ)	5.0
final angle (° 2θ)	100.0
step width (° 2θ)	0.03
time/scan (h)	20
no. of variables	84

* R-p, R-wp and R- F^2 as defined in TOPAS (Bruker AXS)

Table S 2. Atomic coordinates of the 2-1-5 phase ($\text{Cu}_3(\text{CH}_3\text{COO})_4(\text{OH})_2 \cdot 5\text{H}_2\text{O}$) at ambient conditions.

Atom	Wyck.	Site	S.O.F.	x/a	y/b	z/c	B /Å ²
Cu1	4e	1	1	0.1920(3)	0.3387(3)	0.3750(4)	1.14(5)
Cu2	4e	1	1	0.6851(3)	0.8253(3)	0.6783(4)	1.14(5)
Cu3	4e	1	1	0.7401(4)	0.8118(3)	0.3995(5)	1.14(5)
O1	4e	1	1	0.304(1)	0.3131(8)	0.289(1)	2.77(17)
O2	4e	1	1	0.239(1)	0.0257(8)	0.899(2)	2.77(17)
O3	4e	1	1	0.794(1)	0.801(1)	0.580(2)	2.77(17)
O4	4e	1	1	0.482(1)	0.071(1)	0.805(1)	2.77(17)
O5	4e	1	1	0.835(1)	0.280(1)	0.358(1)	2.77(17)
O6	4e	1	1	0.291(1)	0.556(1)	0.630(1)	2.77(17)
O7	4e	1	1	0.810(1)	0.081(1)	0.310(1)	2.77(17)
C1a	4e	1	1	0.542(2)	0.805(2)	0.854(2)	1.43(14)
C2a	4e	1	1	0.440(3)	0.835(4)	0.892(4)	1.43(14)
O1a	4e	1	1	0.603(1)	0.747(1)	0.927(1)	1.43(14)
O2a	4e	1	1	0.562(4)	0.839(2)	0.750(2)	1.43(14)
C1b	4e	1	1	0.333(2)	0.001(2)	0.471(2)	1.43(14)
C2b	4e	1	1	0.365(3)	-0.099(2)	0.476(4)	1.43(14)
O1b	4e	1	1	0.324(1)	0.042(1)	0.364(1)	1.43(14)
O2b	4e	1	1	0.317(2)	0.039(3)	0.574(2)	1.43(14)
C1c	4e	1	1	0.099(2)	0.140(1)	1.066(2)	1.43(14)
C2c	4e	1	1	0.021(3)	0.118(2)	1.148(3)	1.43(14)
O1c	4e	1	1	0.060(1)	0.145(1)	0.946(1)	1.43(14)
O2c	4e	1	1	0.201(2)	0.154(2)	1.121(3)	1.43(14)
C1d	4e	1	1	0.029(2)	0.123(3)	0.588(2)	1.43(14)
C2d	4e	1	1	0.021(4)	0.117(4)	0.447(2)	1.43(14)
O1d	4e	1	1	0.120(1)	0.149(1)	0.657(2)	1.43(14)
O2d	4e	1	1	-0.058(3)	0.101(5)	0.630(4)	1.43(14)

Table S 3. Selected interatomic distances and angles of the 2-1-5 phase ($\text{Cu}_3(\text{CH}_3\text{COO})_4(\text{OH})_2 \cdot 5\text{H}_2\text{O}$) at ambient conditions.

Atoms	Distance	Atoms	Distance	Atoms	Distance	Atoms	Distance
Cu1-O1	1.83(2) Å	Cu2-O1	2.03(1) Å	Cu3-O1	2.01(2) Å	C1a-O1a	1.27(1)
Cu1-O2	2.04(2) Å	Cu2-O3	1.95(2) Å	Cu3-O3	1.90(2) Å	C1a-O2a	1.30(1)
Cu1-O3	2.07(1) Å	Cu2-O2a	1.85(2) Å	Cu3-O1a	1.97(1) Å	C1b-O1b	1.27(1)
Cu1-O1c	1.96(1) Å	Cu2-O1b	1.91(1) Å	Cu3-O1d	2.07(1) Å	C1b-O2b	1.30(1)
Cu1-O1d	2.29(1) Å	Cu2-O2c	2.34(1) Å	Cu3-O2b	2.32(2) Å	C1c-O1c	1.27(1)
Cu1-O2c	2.60(2) Å	Cu2-O1a	2.89(1) Å	Cu3-O2c	2.41(3) Å	C1c-O2c	1.30(1)
C1a-C2a	1.49(1)	C1b-C2b		C1c-C2c		C1d-O1d	1.27(1)
				C1d-C2d		C1d-O2d	1.30(1)
Atoms	Angle	Atoms	Angle				
O1a-C1a-O2a	125(1)	O1c-C1c-O2c	125(1)				
O1b-C1b-O2b	125(1)	O1d-C1d-O2d	125(1)				

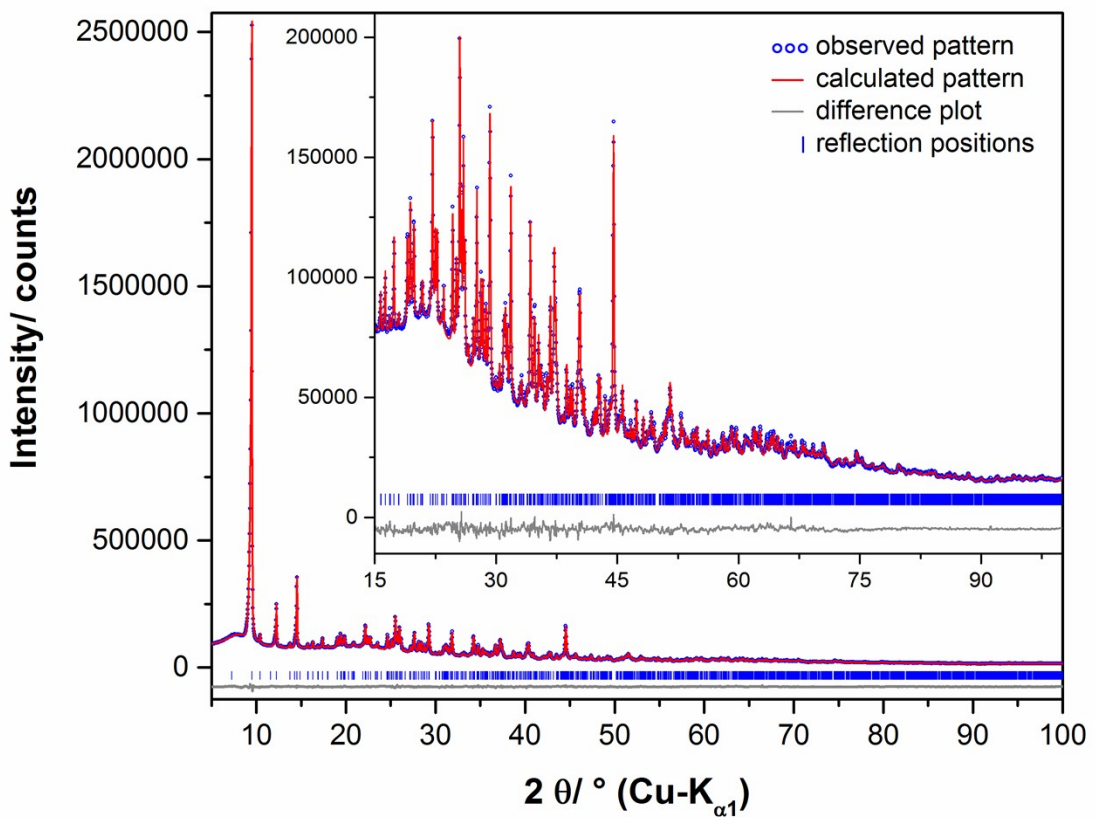


Figure S 2. Scattered X-ray intensities of the 2-1-5 phase ($\text{Cu}_3(\text{CH}_3\text{COO})_4(\text{OH})_2 \cdot 5\text{H}_2\text{O}$) at ambient conditions as a function of diffraction angle 2θ . The observed pattern (circles) measured in Debye-Scherrer geometry, the best Rietveld fit profiles (line) and the difference curve between the observed and the calculated profiles (below) are shown. The high angle part starting at 15.0° in 2θ is enlarged for clarity.

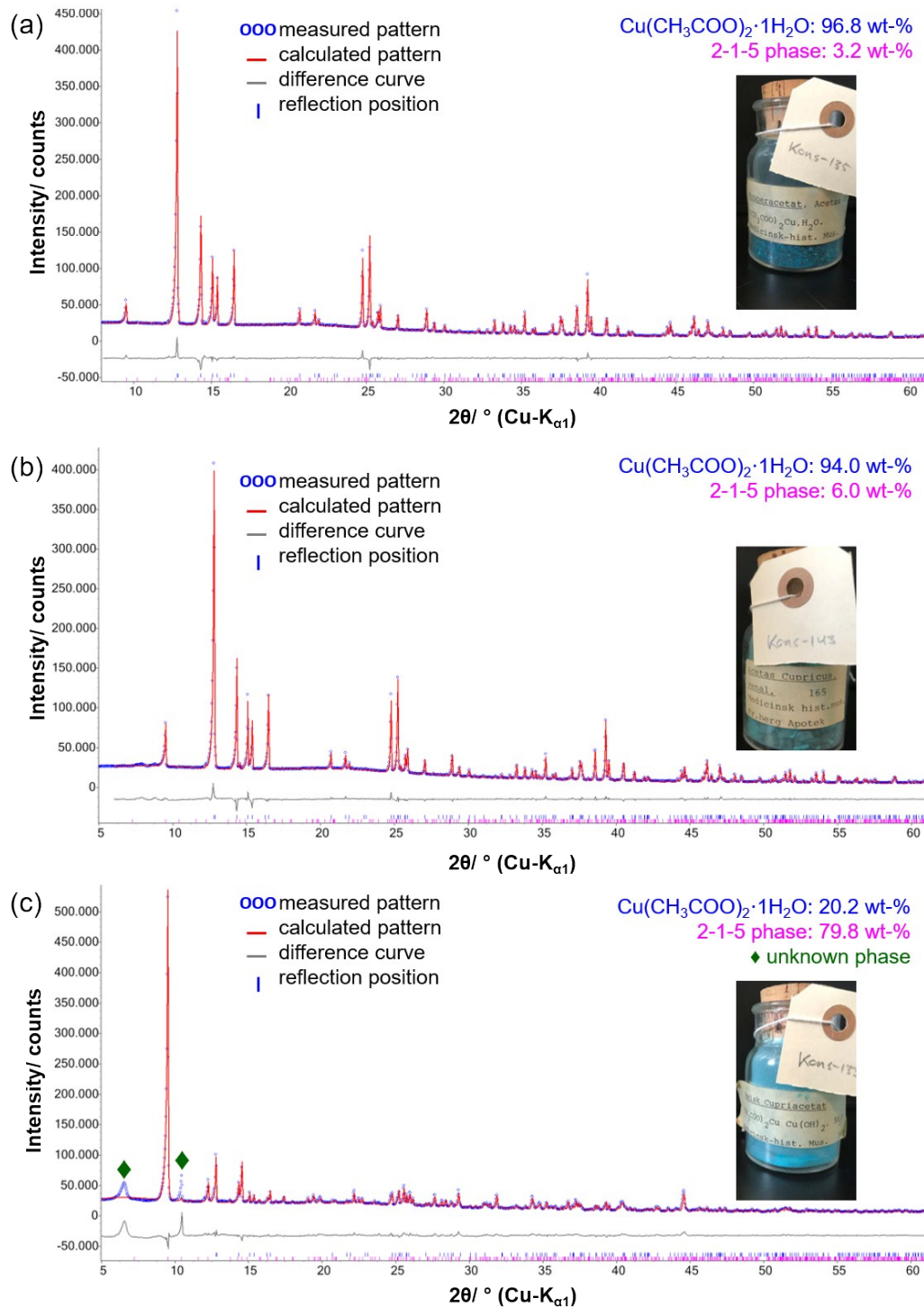


Figure S 3. Graphical results of the quantitative phase analyses of historic pigment samples including photographs of the storage vessels, (a) Kons-135 “Kobberacetat, Acetas Cupric ($\text{CH}_3\text{COO})_2\text{Cu}, \text{H}_2\text{O}$ ”, (b) Kons-143 “Acetas Cupricus Venal” and (c) Kons-133 “Basisk Cupriacetat ($\text{CH}_3\text{COO})_2\text{Cu Cu}(\text{OH})_2, 5 \text{H}_2\text{O}” the given contents of $\text{Cu}(\text{CH}_3\text{COO})_2 \cdot \text{H}_2\text{O}$ and of the 2-1-5 phase for this samples only refer to a relative ration as an undetermined amount of an unknown phase is present, as well.$

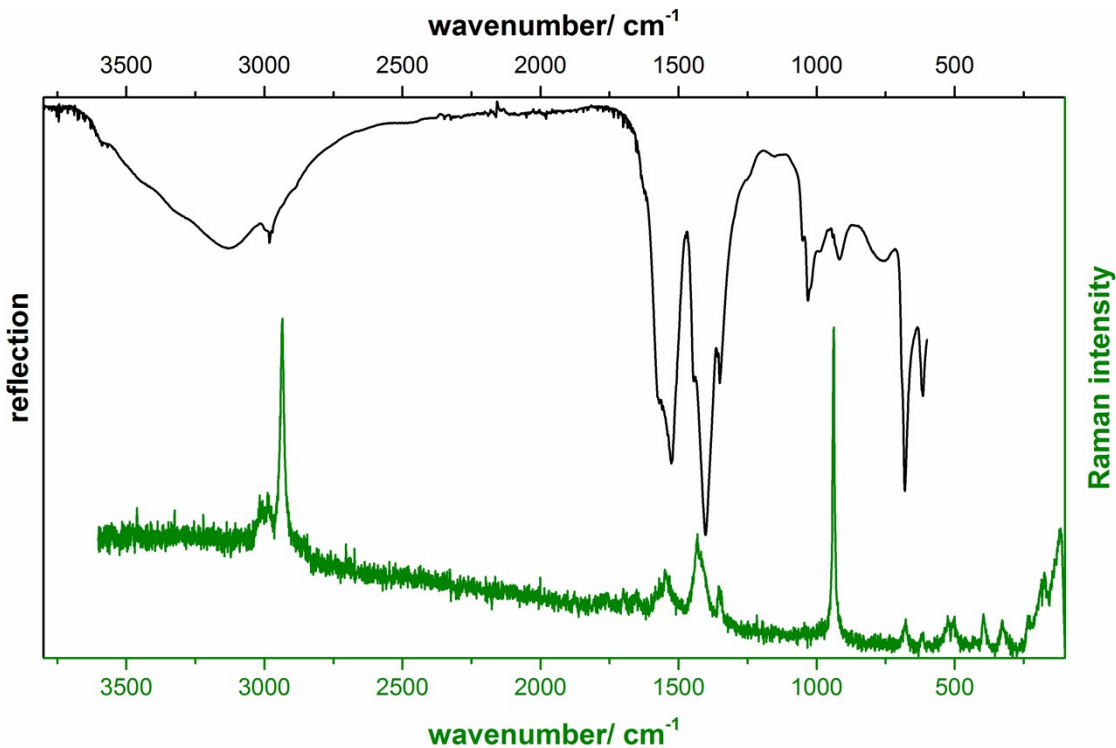


Figure S 4. Raman and FT-IR (ATR) spectrum of the 2-1-5 phase.

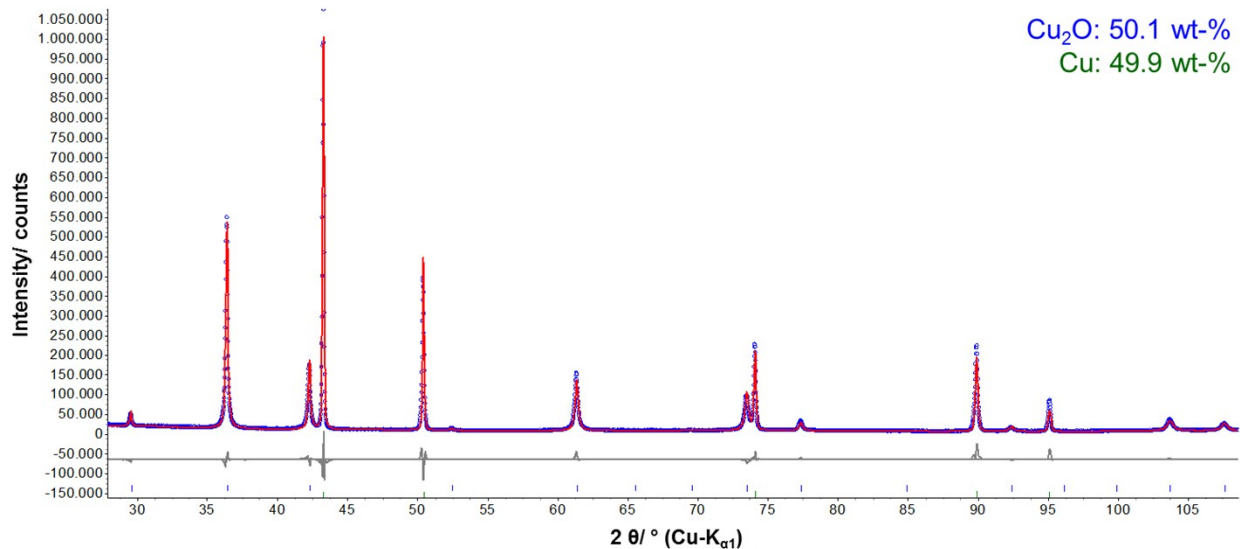


Figure S 5. Quantitative phase analysis of the residue of the 2-1-5 phase after thermal decomposition (*ex-situ*).